

Integrated Petroleum Engineering

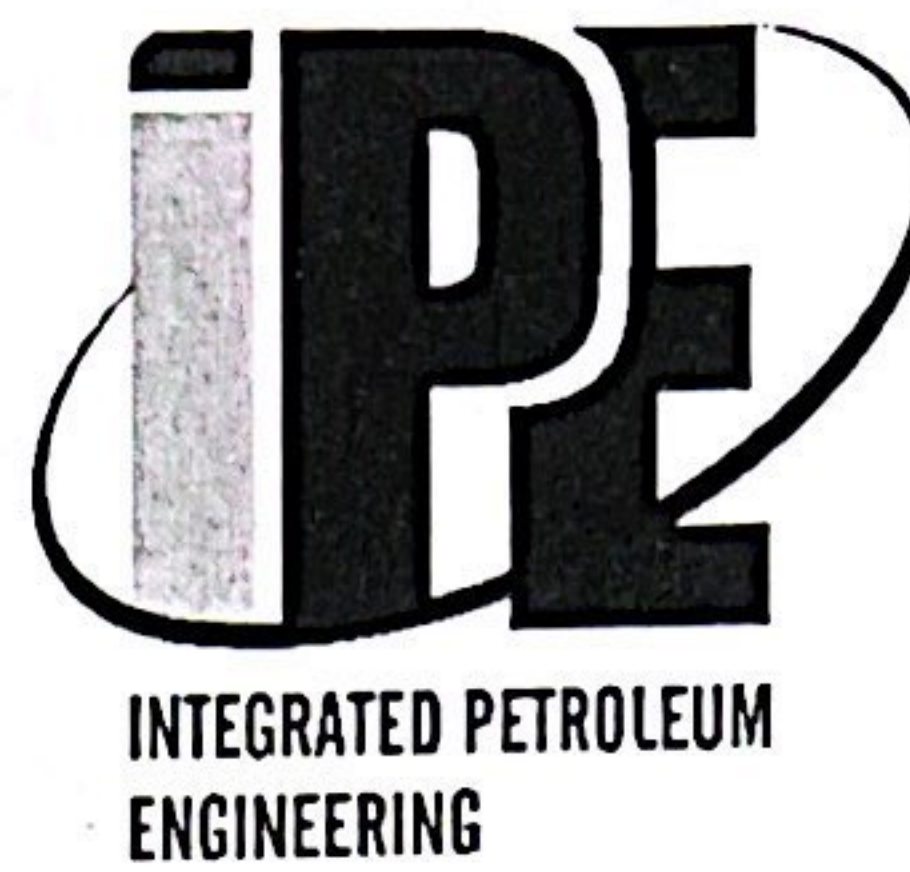
IPE3

Hanoi, October 6, 2022

ISBN: 978-604-76-2595-6



TRANSPORT PUBLISHING HOUSE



Integrated Petroleum Engineering (IPE3)

Hanoi, October 6, 2022

TRANSPORT PUBLISHING HOUSE

TABLE OF CONTENTS

| | | Page |
|---|---|------|
| 1 | Le Hong Quan, Nguyen Thai Hop, Le Minh Hieu, Vu Nam Hai, Hoang Anh Duc. Application of sequence stratigraphy methodology in petroleum prospection and exploration in Block 09-1, Cuu Long basin, continental shelf of Vietnam | 1 |
| 2 | Kim Nguyen Pham Thien, Son Hoang Ky, Dung Doan Thi My, Hung Tran Ngoc The, Pascal Millot. Behind Casing Gas Saturation Determination with Pulsed Neutron Logging in Gas-Filled Boreholes and High Temperature Formations – First Application in Offshore Vietnam | 9 |
| 3 | Trinh Song Bien, Nguyen Anh Duc, Pham Tuan Anh, Tran Ha Minh, Chau Dang Khoa, Nguyen Ngoc Tuan Anh. Intergration of rock typing by hydraulic flow unit concept and borehold image log analysis depositional facies enviroment | 23 |
| 4 | Nguyen Lam Anh, Nguyen Quoc Dung, Pham Dai Nhan, Nguyen Van Trung, Nguyen Van Nga. Hydraulic Fracturing Technology In Tight Oil Reservoir - Case Studies From Upper Ologocene Reservoir At White Tiger Field | 44 |
| 5 | Nguyen Thac Hoai Phuong, Nguyen Quynh Huy, Bui Khac Hung, Doan Thanh Dat, Dong Van Hoang. Applying integrated adaptive model and algorithm with priori information of reservoir parameters for well test data interpretation in Bach Ho field, Cuu Long Basin | 56 |
| 6 | Nguyen Bao Trung Anh. Research and application of polyamine as inhibitor in drilling mud system when drilling in active clay-containing formations | 64 |
| 7 | Van Tu Truong, The Vinh Nguyen, Van Thinh Nguyen, Tien Hung Nguyen, Khac Long Nguyen, Tai Nguyen Trong. Oil and Gas Well Stimulation by Hydraulic Fracturing in the Oligocene of Bach Ho Field. Case study: Hydraulic fracturing for well X-MSP10 | 71 |
| 8 | Truong Nguyen Huu, Tung Phi Manh, Nguyen Van Trung, Nhan Hoang Thinh. Acid treatment of the Basement formation for improved oil rate: A case study of the producer well in the White Tiger field | 83 |
| 9 | Truong Nguyen Huu, W. Bae, X. Nguyen, Nhan HoangThinh. Effect of Fluid Leak-off on Fracture Geometry during Hydraulic Fracturing: A case study in the Lower Miocene Reservoir, White Tiger Field | 91 |

- 10 **Ngo Huu Hai, Nguyen The Vinh, Nguyen Trong Tai.** Potential for producing hydrogen from depleted gas fields with existing production facilities offshore Vietnam 97
- 11 **Quang Nguyen, Tran Anh Tong, Nguyen The Vinh, Truong Van Tu.** Projected FR-PR Conjugate Gradient Algorithm with Stochastic Simplex Approximated Gradient (StoSAG) for Efficient Waterflooding Optimization 107
- 12 **Tran Duy Ngoc Giao, Ta Quoc Dung, Pham Van Hoanh, Le The Ha, Vu Thiet Thach.** Using updated algorithm to built phase diagram for multicomponent hydrocarbon system 115
- 13 **Nguyen The Dzong, Nguyen Lam Anh.** IOR/EOR research & development for Vietsovpetro Joint venture oil fields 127
- 14 **Nguyen Tran Tuan.** Application of rotary – percussion horizontal drilling technology for methane drainage in Khe Cham coal mine, Quang Ninh, Viet Nam 137
- 15 **Nguyen Hai An, Nguyen Hoang Duc, Le Ngoc Son.** Simulation Study On Enhanced Oil Recovery Integration Co₂ Sequestration In Su-Tu-Den Fractured Basement Reservoir 142
- 16 **Ha-Son NGO, Huu-Thanh LE, Ngoc-Tuan TRAN.** Fabrication of nano Selenium in Solution plasma 154
- 17 **Thuy T. L. Bui, Thuan Dinh Dao, Ngoc-Cong Pham.** Fibroin/chitosan based composite preservatives for longan postharvest preservation 162
- 18 **Canh Nguyen Van, Thang Cong Ngoc, Hung Nguyen Tran, Tuan Le Quang.** Modifying Investigation of Nano-silica Additive for Orientating Applications on Enhanced Oil Recovery 173
- 19 **Tho D. Le, Long T. Nguyen, Tuan N. Tran, Thang N. Cong, Hai T. Ngo, Toan V. Vu, Ha M. Nguyen, Hong T. M. Nguyen, Bao T.T. Nguyen, Huong T.T. Tong.** Characterization and Application of Transparent Wood Fabricated from Balsa Wood 181
- 20 **Linh T.Nguyen, Mai Anh T.Nguyen, Ha T.Bui, Duong V.Le, Lan Anh T.Ha.** Influence of the synthesis conditions on the formation of MSU-Z mesoporous material from Vietnamese kaolin and rice husk 188
- 21 **Ngo H Hai, Tran N Trung, Tran V Tung, Dao Q Khoa, Nguyen T Trung, Hoang K Son, Trieu H Truong.** Anomaly Detection for Centifuge Natural Gas Compressor Using LSTM-Based Autoencoder in Hai Thac – Moc Tinh Field, Offshore Vietnam 197



International Conference on Integrated Petroleum Engineering (IPE-2022)

Characterization and Application of Transparent Wood Fabricated from Balsa Wood

Tho D. Le ^{a,*}, Long T. Nguyen ^a, Tuan N. Tran ^a, Thang N. Cong ^a, Hai T. Ngo ^a,
Toan V. Vu ^a, Ha M. Nguyen ^a, Hong T. M. Nguyen ^a, Bao T.T. Nguyen ^b,
Huong T.T. Tong ^{a,*}

(a) Faculty of Oil and Gas, Hanoi University of Mining and Geology

(b) Institute of Physics; Vietnam Academy of Science and Technology

Abstract

Optically transparent wood, which combines optical and mechanical performance, is a new material that is being developed for light-transmitting structures in buildings with the intention of reducing energy usage. One of the most significant challenges to transparent wood production is delignification, which involves removing about 30 – 35 % of the wood tissue to reduce light absorption and refraction mismatch. Removing lignin from wood and then impregnating it with ecofriendly polymers whose refractive index matches that of the cell wall assists in the fabrication of transparent wood. A green and industrially viable process for preparing translucent wood now can be established.

As in the research, we present a simple approach for producing transparent wood from balsa wood while maintaining its three-dimensional structure. The wood chemistry structure was investigated using FTIR measurement. Optical studies revealed that the highest optical transmittance for 1 mm to 3 mm thickness of wood samples was 43 – 70 %. Mechanical testing revealed that translucent wood has higher elastic modulus than delignified wood and natural wood. Transparent wood with high transmittance and improved mechanical qualities has been developed as a promising candidate material for light transmitting construction materials and transparent solar cell windows. This material, on the other hand, exhibits hydrophobic characteristics, allowing for the development of oil/water separation applications.

Keyword: Balsa wood, epoxy-wood, delignified, transparent wood

1. Introduction

Residential and commercial building energy use represents about 40 % of overall energy consumption (T. Mohammed et al. 2013, P. Nejat et al. 2015, M. Santamourisa et al. 2021). Furthermore, energy demand for buildings is expected to rise much further in the future (S. Haddad et al. 2020). Glass is an intriguing building material in this context, owing to its great optical transmission. It is used in windows and rooftops to transfer sunlight for illumination purposes, with the added benefit of lowering electrical energy use. Even structural grades of glass, however, are too fragile for large load-bearing structures and may cause glare (M. Achintha et al. 2016, M. Santamouris et al. 2020, I. Konstantzos et al. 2015). Furthermore, glass has a rather high thermal conductivity, which frequently results in thermal leakage. These properties limit the application of glass materials. As a result, alternative construction materials with favorable mechanical properties, sunlight-controlling properties, and even light-emitting properties are being developed (A. Borisuit et al. 2015).

Wood is a material that is commonly used in the construction industry. Wood has great mechanical qualities in relation to its cost because of its unique structure and natural growth process. These characteristics include great strength, long durability, high moisture content, and a high specific gravity. Wood is divided into two classes based on its structure, availability, and geographical variations. There are two types of wood: soft wood and hard wood. The porosity of soft wood is very large. Hard wood has a higher density and a denser structure

* Corresponding author.

E-mail address: tongthithanhhuong@humg.edu.vn,
leductho.tk@gmail.com

than soft wood (C.E. Byrne et al. 1997). However, the hierarchical structure of both soft and hard woods is identical and the wood has comparable cell orientation (J. Shen et al. 2000).

One distinctive quality of a wood is its structural anisotropy. This is caused by how the vertical channels across the wood's cells are arranged. The primary component of wood cells is cellulose, a long chain of polysaccharide molecules. Hemicellulose, a kind of polysaccharide chain with a lower molecular weight, is also a component of cellulose. The other important component present in wood is lignin. About 25% of the wood structure is made up of it. It primarily functions as glue to link all the wood cells together. Lignin also gives the wood a high degree of stiffness and toughness. Cellulose, hemicellulose, and lignin are the three primary substances that make up wood, as was already explained. Lignin has a very dark color, in contrast to the colorless cellulose and hemicellulose. As a result, its dark color causes light to disperse over the visible spectrum. Bleaching the wood, which removes the lignin and pulp, is one method of making it transparent. Because of the color across the wood's pores is left in place, polymer that can offer strength and transparency is impregnated into the wood's downwards pores. Transparent wood has been successfully created in a number of recent attempts. However, the method for creating transparent wood that has thus far been developed is difficult and maybe harmful to the environment (M. Zhu et al. 2016).

Recently, transparent wood, a material with innovative applications, has remained popular. The combination of load-bearing and functional properties in transparent wood structures has been made possible by new procedures for wood functionalization (L.A. Berglund et al. 2018). With characteristics including high transmittance, tailored haze, light wave directing properties, attractive mechanical and thermal insulation properties, and more, transparent wood is an excellent option for construction materials (Y. Li et al. 2018, E. Vasileva et al. 2017).

In another site, oil pollution in the water environment is a result of production, exploitation, and transportation activities that have a negative impact on the ecosystem. Therefore, various materials have been investigated in order to solve the increasing worry of separating these spilled oils from a great amount of oilywater. Actually, hydrophobic materials have a low surface energy and are oil-repellent for light oil. However, due to the high viscosity and sticky nature of crude oil, they are quickly and seriously polluted during the separation of crude oil/water mixtures. As a result, it is critical and necessary to develop a system for high-efficiency oil/water separation.

In this work, transparent wood is created and modified to improve its mechanical and optical properties. The intention is to use a two-step synthesis procedure to create transparent wood from balsa wood. In this article, we describe the synthesis of optically semi-transparent wood that has an optical transmittance of 70 %. The mechanical and microstructural properties have also been investigated in detail. The preliminary material's hydrophobicity was examined, offering up a new application option in the field of environmental treatment.

2. Experimental

2.1 Materials

Balsa wood was purchased from San Ho Timber Pte Ltd, Singapore. The wood sample was cut into size of $30 \times 30 \text{ mm}^2$ (longitudinal \times radial). Sodium chloride (NaClO_2) was from Sigma Aldrich. Sodium acetate (CH_3COONa) and acetone were purchased from Xilong Scientific Co., Ltd., China. Acetic acid was from Duc Giang Co. Ltd., Vietnam. Acrylic epoxy resin and hardener epoxy resin were provided by JDiction.

2.2 Preparation of Delignified Wood

The balsa wood samples were chemically extracted with NaClO_2 with acetate buffer solution of pH 4.6 at 80°C . The reaction times were 6 – 24 hours. Delignified wood samples were cleaned in deionized water. After that they were dehydrated first with pure ethanol and then with 1:1 mixture of ethanol and acetone. Every step was repeated thrice.

2.3 Preparation Transparent Wood

The porous delignified wood was impregnated with epoxy solution (the ratio of acrylic epoxy resin/hardener epoxy resin is 3/1) and dried at 80°C for 24 hours. The translation wood samples were thoroughly washed with acetone twice to remove extra epoxy.

2.4 Characterizations

Changes in the surface chemistry of the wood before and after the treatment were analyzed using Fourier transform infrared spectroscopy (IRAffinity-1, Shimadzu). The FTIR spectra were recorded using the KBr pellet method, ranging from 4000 to 500 cm^{-1} at 4 cm^{-1} resolutions for 32 scans. The transmittance was determined

using a Shimadzu UV-2600 ultraviolet-visible spectrometer with a wavelength ranging from 300 nm to 800 nm. For practical applications mechanical characterizations were also performed. The tensile strength, elastic modulus according to ASTM D638, which were performed on a Zwick Z2.5 tractor (Germany). The samples were tested at room temperature with dimensions of 50 mm x 30 mm. All experiments were repeated 3 times to get the mean value. Water contact angles were measured using a Ramé-hart Contact Angle Goniometer model 250. Through out, the wettability and absorption capability of water can be predict.

3. Results and Discussion

3.1 Transparent Wood

Balsa wood was used as the raw material. The transparent wood was created using the synthetic process shown in Fig 1. In the experiment, the polymer with a matched refractive index was infiltrated into the wood substrates. The chemical treatment of natural wood resulted in a large decrease in lignin and hemicellulose content, but only a slight decrease in cellulose content, showing that cellulose is the primarily retained component following the treatment. Fig. 1 illustrates the remarkable transparency of transparent wood generated by infiltrating epoxy into intact delignified wood.

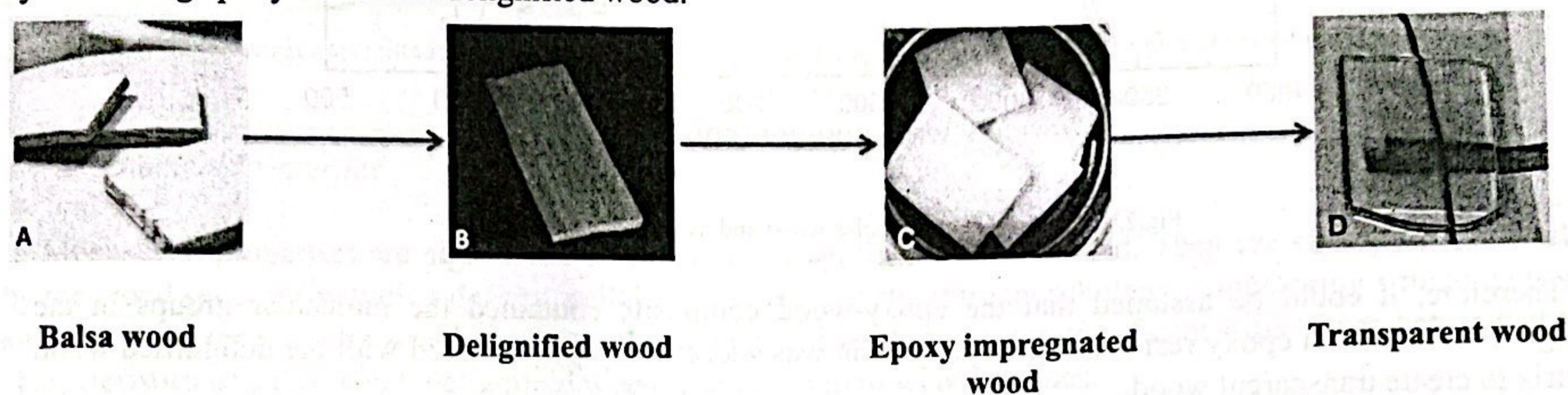


Figure 1. Synthetic method and digital photograph of the transparent wood.

3.2 Fourier Transform Infrared (FTIR) Characterization

The FTIR analysis for samples of untreated balsa wood, delignified wood, and transparent wood is shown in Fig. 2. It is obvious that from balsa wood to transparent wood, the absorption intensity at 3332 cm^{-1} decreases. The reduction of hydroxyl groups in the substance is the explanation of this change in intensity. Epoxy is thus carrying an ether group and an unsaturated $\text{C}=\text{C}$ double bond due to the presence of the vinyl monomer. Through the process of free-radical polymerization, this becomes grafted onto the wood matrix. Epoxy-wood composite (transparent wood) is formed as a result of a chemical compounding between the polymer and the wood matrix.

According to the spectral results, apart of peaks at 3332 cm^{-1} and 2927 cm^{-1} were also observed in most of samples, which are identified as $\text{O}-\text{H}$ stretching absorption and $\text{C}-\text{H}$ absorption bands, respectively, for cellulose and hemicellulose. On the other hand, the spectrum shown that lignin was removed from the balsa wood sample. In contrast to the untreated wood, the aromatic ring structure on the lignin-type sample at 1509 cm^{-1} (Fig. 2a) almost disappeared for the delignified samples (Fig. 3b, c, d). Furthermore, in the delignified samples, no signal of valence fluctuations appeared at 1242 cm^{-1} . This is the signal for $\text{C}-\text{O}$ in a G_Ring (guaiacyl unit) $\text{C}=\text{O}$ stretching structure. In contrast to the untreated wood, the delignified wood shown the absence of lignin band, which further confirms that the lignin present in the wood is removed. As is well known, lignin is a heteroaromatic biopolymer formed of sinapyl, coniferyl, and p-coumaryl alcohols as its primary monomers. Ether and $\text{C}-\text{C}$ linkages are used to connect these three monomers. When lignin interacts with NaClO_2 (B. Liu, et al. 2020), it undergoes an obvious oxidative conversion that leads to oxidative depolymerization, which breaks down chemical bonds and generates low-molecular-mass products (A. J. Ragauskas et al., 2014). Oxidative cracking can occur when aromatic rings, $\text{C}-\text{C}$ bonds, aryl ether links, or other lignin polymer linkages break. Consequently, lignin was removed from natural wood during oxidation process with NaClO_2 .

For epoxy-wood samples, the absorption peaks epoxy resin include the symmetric stretching vibration of the $\text{C}-\text{H}$ group on CH_3 at a wavelength of 2965 cm^{-1} , the antisymmetric stretching vibration of the $\text{C}-\text{H}$ group on CH_3 at $2865, 1606\text{ cm}^{-1}$ (Fig. 2e). Besides, it includes the asymmetric vibration band of the benzene ring skeleton at 1491 cm^{-1} , the scissor swing vibration of CH_3 at 583 cm^{-1} , the stretching vibration of aliphatic ether $\text{C}-\text{O}-\text{C}$ at 1246 cm^{-1} , the out of plane deformation of para-substituted benzene ring of $=\text{CH}$ at 825 cm^{-1} . It can be seen from the figure that the infrared spectrum of the transparent wood samples obtained by impregnation of epoxy resin has not only the characteristic absorption peak of delignified wood, but also the characteristic peak of epoxy resin.

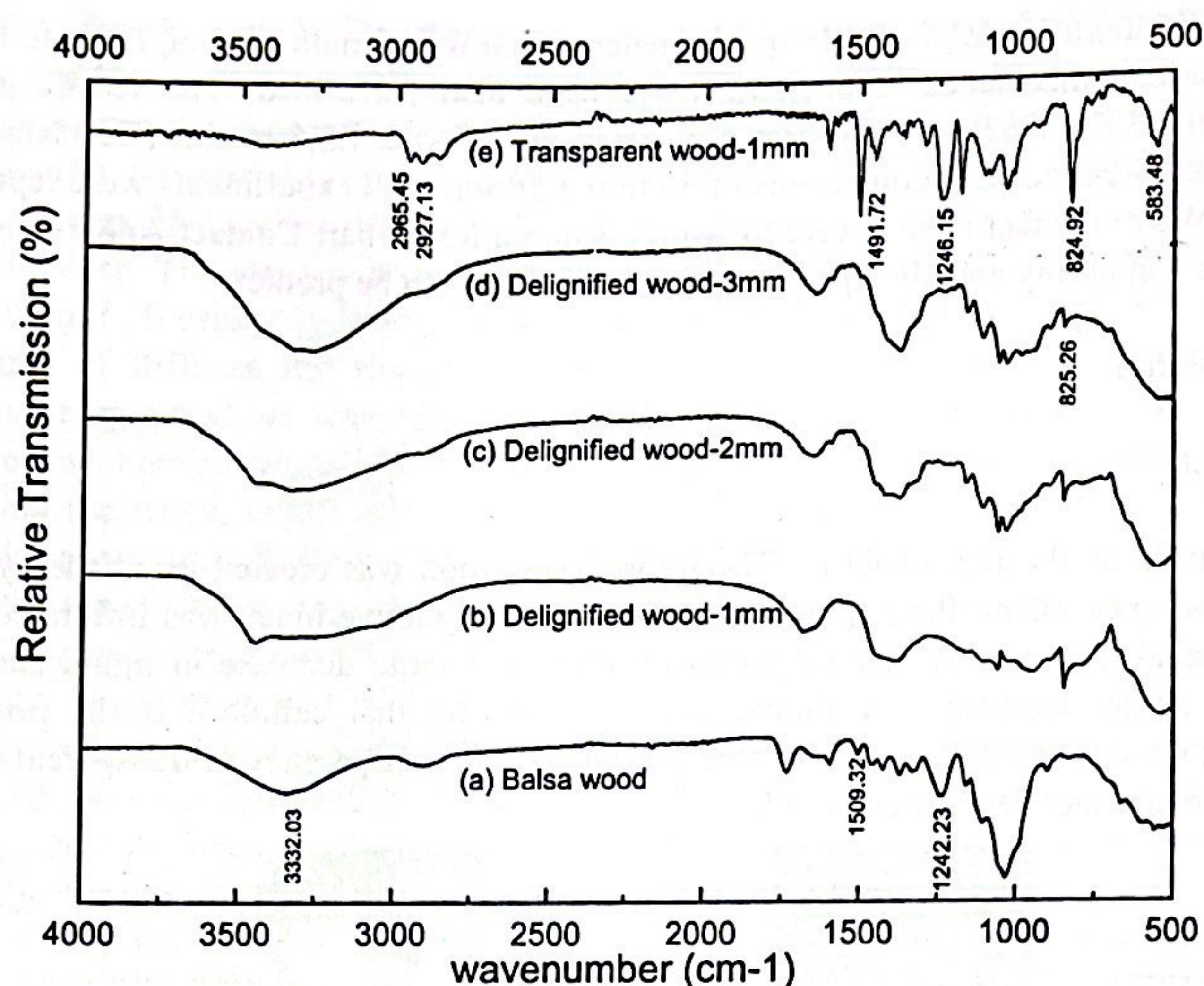


Fig.2. FTIR spectra of the balsa wood and modified wood samples

Therefore, it could be assumed that the epoxy-wood composite contained the molecular groups in the delignified wood and epoxy resin, and the epoxy resin was successfully polymerized with the delignified wood matrix to create transparent wood.

3.3. Optical Transmittance

The optical transmittance for untreated balsa wood, delignified wood, and transparent wood of variable thickness (1 - 3 mm) across a wide wavelength range of 300 - 800 nm are shown in Fig. 3. It is noticeable that the balsa wood has almost not transmission. This is due to the presence of cellulose, lignin and hemicellulose, which absorb most of the light. In cases of epoxy, shows the highest transmittance as 90 %. Besides, the delignified wood still shows a low transmission as 8 % above 600 nm. In contrast the optimized transparent wood samples exhibit a transmission value as high as 70 % above 600 nm. Furthermore, as the thickness of the transparent wood varies, the percentage of transmission also differs. According to Fig. 3, the transmittance decreases as the thickness of the sample increases. A transmittance of 70 % was obtained for transparent wood with a thickness of 1 - 2 mm, while a transmittance of 43 % was obtained for transparent wood with a thickness of 3 mm. This variation in transmittance is result of the fact that when light is transmitted, it is attenuated owing to absorption and scattering. As a result, with a higher thickness, light has a longer pathway resulting lower transmittance.

As can be seen, the material's transmittance may well be modified based on variations in fabrication conditions and the removal of lignin from the natural wood. The luminance of the transparent wood can be controlled. This property enhances the material's advantage over traditional glass. Glass has a high transmittance (80 – 90%) depending on the composition, making brightness adjustment challenging (J. Dziedzic et al., 2017). Because of their simplicity of luminance control and better plastic strength, transparent wood may provide a wide variety of quality application.

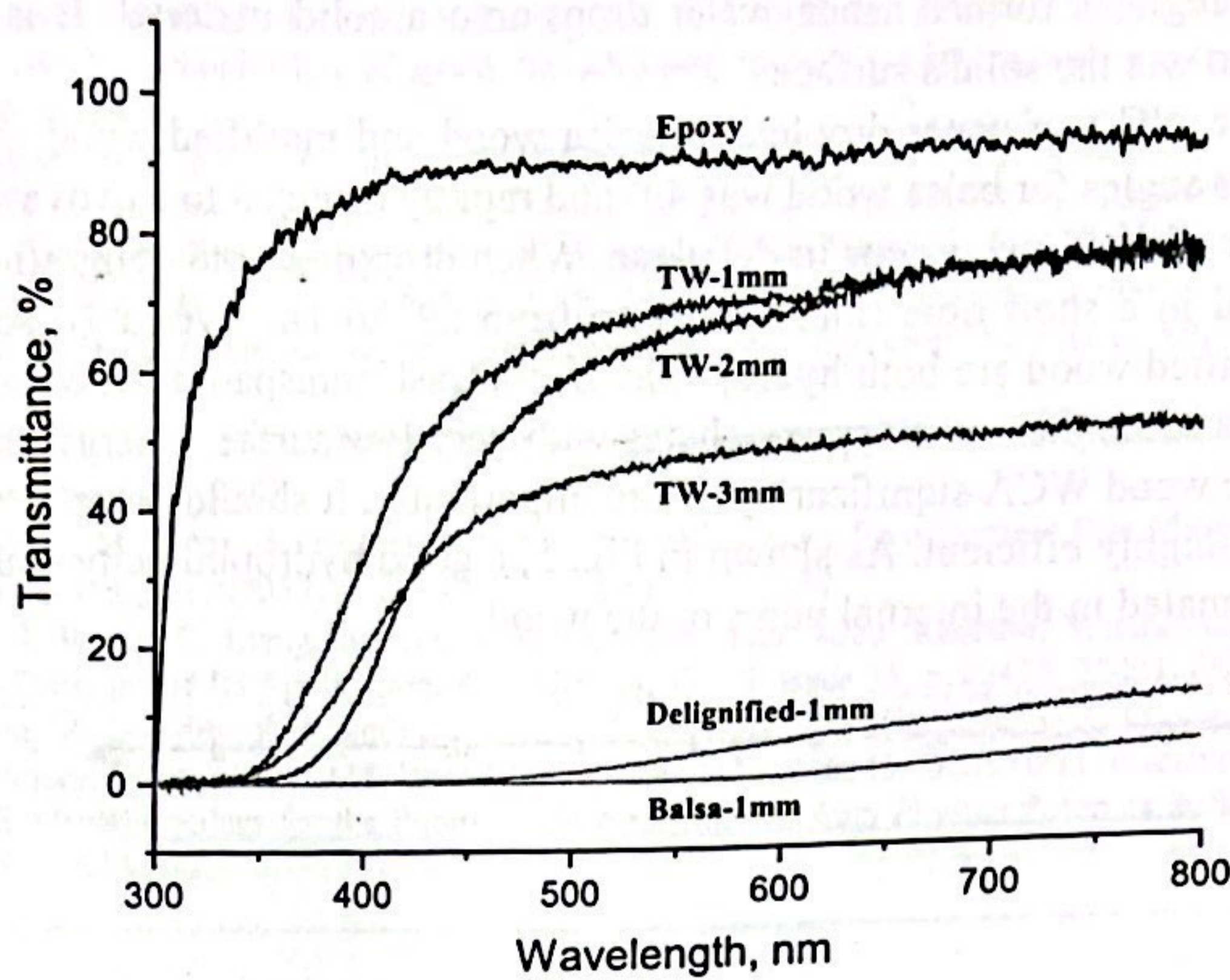


Fig. 3. UV-Visible optical transmittance of balsa wood, delignified wood, transparent wood (TW) samples of varying thickness (1 - 3 mm) and epoxy.

3.4. Mechanical Properties

Mechanical properties are significant for a variety of applications considered. They are strongly influenced by the wood species (including density, cellulose content, cell structure morphology, annular ring structure etc.) and the anisotropy of the wood structure. According to Fig. 4, there are significant differences between the characteristics of balsa wood, delignified wood, and transparent wood samples.

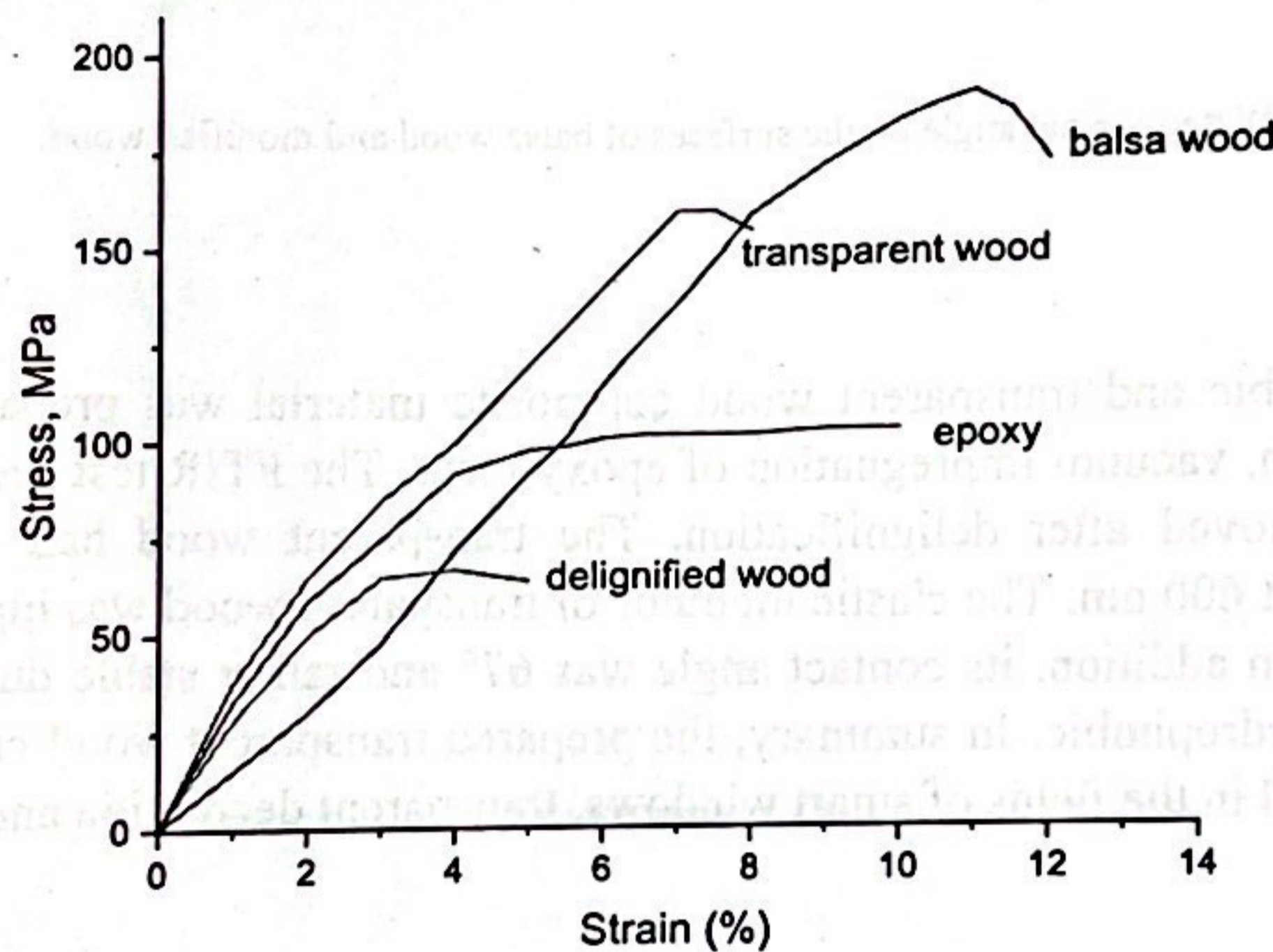


Fig. 4. Stress and strain relationship of balsa wood, delignified wood, transparent wood samples and epoxy

It is clearly observed that the transparent wood is much stronger with an elastic modulus is of 2.4 GPa than that of the delignified wood whose elastic modulus is 2.05 GPa, balsa wood of 1.65 GPa and epoxy with an elastic modulus of 2.1 GPa. Balsa wood has a low elastic modulus because of the weak hydrogen bonding in materials. Delignified wood has a lower elastic modulus than transparent wood because there are not any strong hydrogen bonds connecting the cell walls together. The amount of cellulose that can form hydrogen bonds in the cell walls of the wood determines its mechanical properties. When the lignin in delignified wood was largely removed, many pores were formed. After the epoxy resin was fully impregnated, epoxy resin and wood were united and form hydrogen bonds. The impregnation of resin make transparent wood has the great elastic modulus due to strong hydrogen bonds are created across the cell walls of transparent wood between the polymer and the hydroxyl groups on the cellulose. As a result, it is expected that the inter-cellulose-epoxy bonding in transparent wood will significantly improve the material's toughness and hardness, providing the possibility for its application in a broad field.

3.5. Hydrophobicity of Wood

The aim of this study is to improve the hydrophobicity by epoxy surface modification. The hydrophobicity could be represented by water contact angle (WCA). Wettability and wood-based composites are intricately

related. The water contact angle is formed when water drops onto a solid material. It is a critical metric to evaluate the liquid's ability to wet the solid's surface.

Fig. 5 is a diagram of the WCA of water droplets on balsa wood and modified wood. As can be seen from this figure, the initial contact angles for balsa wood was 42° and rapidly dropped to 27° over a 10 seconds period because of the large amount of hydroxyl groups in cellulose. When dropping onto delignified wood, the droplet is absorbed and disappeared in a short time (rapidly reduce from 29° to 18° over a 10 seconds period). This means that balsa and delignified wood are both hydrophilic. In contrast, transparent wood presents a stability of contact angles. After modification, there were epoxy chains with very low surface energy grafted onto the wood surface, which increased the wood WCA significantly. More importantly, it should be pointed out that the epoxy modification of the wood is highly efficient. As shown in Fig. 5, a good hydrophobicity could be realized when epoxy was filled and impregnated in the internal pores of the wood.

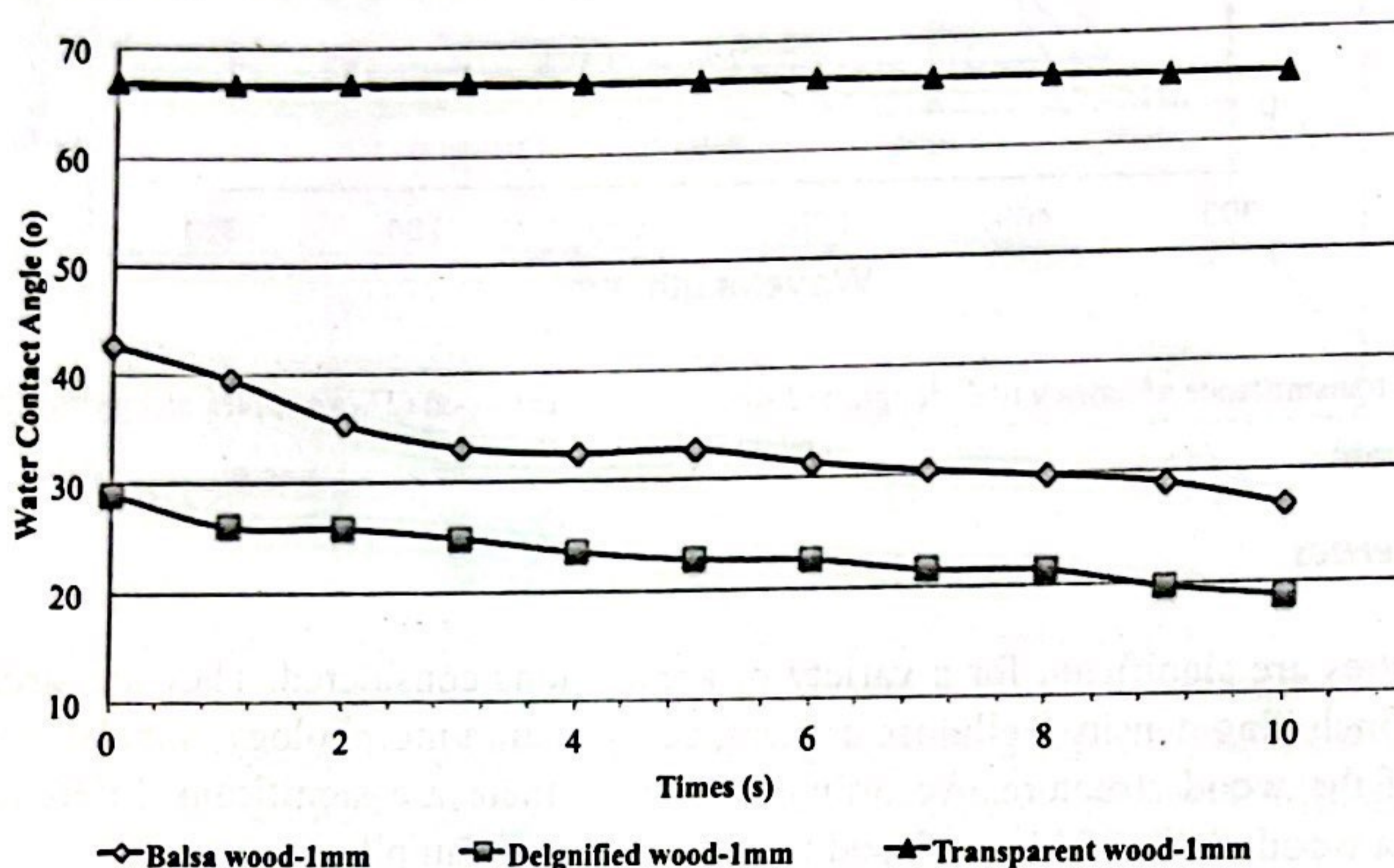


Fig.5. Water contact angle on the surfaces of balsa wood and modified wood.

4. Conclusions

In conclusion, a hydrophobic and transparent wood composite material was prepared through two steps: sodium chlorite delignification, vacuum impregnation of epoxy resin. The FTIR test revealed that the lignin of the wood was basically removed after delignification. The transparent wood had a relatively high light transmittance reaching 70 % at 600 nm. The elastic modulus of transparent wood was higher than that of natural wood and delignified wood. In addition, its contact angle was 67° and rather stable during 10 seconds, which proved that its surface was hydrophobic. In summary, the prepared transparent wood created from balsa wood had broad application potential in the fields of smart windows, transparent decoration and oil/water separation.

Acknowledgments

This research has done with the financial support from Vietnam Academy of Science and Technology under the project VAST01.04/18-19

References

- T. Mohammed, R. Greenough, S. Taylor, L. Ozawa-Meida, A. Acquaye; 2013. Operational vs. embodied emissions in buildings—A review of current trends, *Energy Build.* Vol 66, p. 232 - 245. DOI: 10.1016/j.enbuild.2013.07.026.
- P. Nejat, F. Jomehzadeh, M.M. Taheri, M. Gohari, M.Z. Muhd; 2015. A global review of energy consumption, CO₂ emissions and policy in the residential sector (with an overview of the top ten CO₂ emitting countries), *Renew. Sustain. Energy Rev.* Vol. 43, p. 843 – 862. DOI: 10.1016/j.rser.2014.11.066.
- M. Santamourisa, K. Vasilakopouloub; 2021. e-Prime-Advances in Electrical Engineering, Present and future energy consumption of buildings: Challenges and opportunities towards decarbonisation, *Electronics and Energy*, Volume 1, p. 100002. DOI: 10.1016/j.prime.2021.100002
- S. Haddad, A. Barker; 2020. On the potential of building adaptation measures to counterbalance the impact of climatic change in the tropics, *Energy and Buildings*, Vol. 229, p. 110494. DOI: 10.1016/j.enbuild.2020.110494.
- M. Achintha, 2016. Sustainability of glass in construction, *Sustain. Constr. Mater.* Woodhead, in J.M. Khatib (2nd Ed.), p. 79–104. DOI: 10.1016/B978-0-08-100370-1.00005-6.
- M. Santamouris; 2020. Recent progress on urban overheating and heat island research. Integrated assessment of the energy, environmental, vulnerability and health impact. Synergies with the global climate change, *Energy Build.*, Vol. 207, p. 109482, DOI: 10.1016/j.enbuild.2019.109482.
- I. Konstantzos, A. Tzempelikos, Y.C. Chan, 2015. Experimental and simulation analysis of daylight glare probability in offices with dynamic window shades, *Build. Environ.*, Vol. 87, p. 244 - 254. DOI: 10.1016/j.buildenv.2015.02.007.
- A. Borisuit, F. Linhart, J.-L. Scartezzini, M. Münch, 2015. Effects of realistic office daylighting and electric lighting conditions on visual

- comfort, alertness and mood; *Light. Res. Technol.*, Vol. 47, p. 192–209. DOI: 10.1177/1477153514531518.
- C. E. Byrne, D.C. Nagle, 1997. Carbonization of wood for advanced materials applications, *Carbon*, Vol. 35, p. 259 - 266. DOI: 10.1016/S0008-6223(96)00136-4.
- J. Shen, J. Zhou, O. Vazquez, 2000. Experimental Study of Optical Scattering and Fiber Orientation Determination of Softwood and Hardwood with Different Surface Finishes, *Appl. Spectrosc.* Vol 54, p. 1793 - 1804. DOI: 10.1366/0003702001948899.
- M. Zhu, J. Song, T. Li, A. Gong, Y. Wang, J. Dai, Y. Yao, W. Luo, D. Henderson, L. Hu, Highly, 2016. Highly Anisotropic, Highly Transparent Wood Composites, *Adv. Mater.*, Vol. 28, p. 5181 - 5187. DOI: 10.1002/adma.201600427.
- L.A. Berglund, I. Burgert, 2018. Bioinspired Wood Nanotechnology for Functional Materials, *Adv. Mater. P.* 170 - 285. DOI: 10.1002/adma.201704285.
- Y. Li, Q. Fu, X. Yang, L.A. Berglund, 2018. Transparent wood for functional and structural applications, *Phil. Trans. A.*, Vol. 376, p. 20170182. DOI: 10.1098/rsta.2017.0182.
- E. Vasileva, Y. Li, I. Sychugov, M. Mensi, L. Berglund, S. Popov, 2017. Lasing from Organic Dye Molecules Embedded in Transparent Wood, *Adv. Opt. Mater.* Vol. 5, p. 1700057. DOI: 10.1002/adom.201700057.
- B. Liu, C. Qin, F. Zhang, S. Wang, C. Liang, S. Nie, S. Wang and S. Yao, 2020. Reaction Mechanism of Phenolic Lignin and High Concentration Chlorine Dioxide and Its Application, *ACS Omega*, Vol. 5, Issue 35, p. 22475–22481. DOI: 10.1021/acsomega.0c03028.
- J. Ragauskas, G. T. Beckham, M. J. Bidy, R. Chandra, F. Chen, M. F. Davis, C. E. Wyman, 2014. Lignin Valorization: Improving Lignin Processing in the Biorefinery. *Science*, Vol. 344, Issue 6285, p. 1246843–1246843. DOI: 10.1126/science.1246843.
- J. Dziedzic, M. Inglot, 2017. Ultrathin Glass for the Photovoltaic Applications, *Acta Physica Polonica Series A*, Vol. 132, Issue 1, p. 176-178. DOI: 10.12693/APhysPolA.132.176.